Original Scientific Paper https://doi.org/10.24867/GRID-2026-p66

Development and Characterization of a Functional UV-Photopolymerized PEGDA/PETMP/BMEP Hydrogel Adsorbent for Methylene Blue Removal from Aqueous Media

Betul Eymur Donmez [1,2]
Aslı Beyler Cigil [3]

[1] Gazi University, Graduate School of Natural and Applied Sciences, Department of Advanced Technologies, Ankara, Türkiye
[2] Middle East Technical University, Central Laboratory, Ankara, Türkiye
[3] Gazi University, Vocational School of Technical Sciences, Department of Chemistry and Chemical Processing Technologies, Ankara, Türkiye

ABSTRACT

Highly colored effluents from printing and related industries are an environmental concern because many colorants persist in aqueous environments and resist conventional biological treatment. In this study, a phosphate-functional hydrogel was prepared via UV photopolymerization and evaluated as an adsorbent for methylene blue (MB), a model cationic dye. The network was formed by UV-induced thiol–(meth)acrylate reactions of poly(ethylene glycol) diacrylate (PEGDA), the tetrafunctional thiol pentaerythritol tetrakis(3-mercaptopropionate) (PETMP), and the phosphate-containing comonomer bis[2-(methacryloyloxy)ethyl] phosphate (BMEP; about 10 wt% of the monomers), which was intended to introduce ionizable sites for interaction with MB. A BMEP-free PEGDA/PETMP hydrogel with the same PEGDA-to-solvent ratio and thiol:(meth)acrylate molar ratio (0.78:1) served as a control. Both hydrogels were characterized by Fourier-transform infrared spectroscopy (FTIR), thermogravimetric analysis (TGA), and swelling measurements, while dried Hfunc was also examined by scanning electron microscopy (SEM). MB removal from 10 mg L^{-1} solutions was followed by UV–Vis spectrophotometry as a function of contact time. FTIR spectra showed differences in the C-H and fingerprint regions, consistent with compositional differences between the formulations. After 24 h in deionized water, the swelling ratio was 55.5% for the control and 65.1% for the BMEP-containing hydrogel. After 24 h in 50 mL of 10 mg L^{-1} MB, removal reached 80.8% for the BMEP-containing hydrogel and 27.0% for the control. Under the conditions examined, the BMEP-containing formulation showed substantially greater MB removal than the BMEP-free control. These results indicate the potential of UV-curable phosphate-functional hydrogels as adsorbents for cationic dyes, with possible relevance to colored aqueous streams from printing and related processes.

KEY WORDS
UV photopolymerization, thiol–acrylate hydrogel, PEGDA, PETMP, BMEP, phosphate-functional hydrogel, methylene blue, adsorption

1. Introduction

The discharge of intensely colored industrial effluents is an environmental concern because many synthetic colorants persist in aqueous environments and are difficult to remove by conventional treatment processes. Printing operations are one such source: water-based inks may remain dispersed or dissolved in process water, particularly during equipment cleaning and color-change procedures, producing strongly col-

ored effluents with complex organic content. Recent work on printing wastewater has emphasized the need for efficient color-removal strategies, including adsorption-based approaches (Kara et al., 2026).

Adsorption is widely investigated for removing dyes and other colored contaminants because of its operational simplicity and its applicability to compounds that are not readily biodegradable. Hydrogels are particularly attractive adsorbents: their three-dimensional crosslinked networks absorb substantial amounts of water while retaining structural integrity, and their composition, crosslink density, swelling behavior, and functional groups can be tailored to control interactions with dissolved contaminants (Yang et al., 2022). Hydrogel-based materials have accordingly been studied for the adsorption of organic dyes and other colorants from aqueous media (Pereira et al., 2021; Kara et al., 2026).

Methylene blue (MB) is a water-soluble cationic dye widely used as a model contaminant for evaluating adsorbent performance. Its strong visible absorption enables quantitative monitoring by UV-Vis spectrophotometry, and its cationic character makes it well-suited to probe interactions with negatively charged or ionizable groups (Yang et al., 2022). Depending on the adsorbent, MB uptake may involve electrostatic attraction, hydrogen bonding, or both. MB has also been discussed in the context of effluents from paper, printing, and dyeing industries (Rafatullah et al., 2010). In the present work, however, MB is used as a model cationic dye rather than as a representative printing pigment, so that the behavior of the developed hydrogel can be evaluated under controlled conditions.

Poly(ethylene glycol) (PEG)-based acrylate and methacrylate monomers provide a versatile platform for hydrophilic crosslinked networks, and multifunctional thiols can participate in UV-induced thiol-ene/thiol-acrylate network formation with (meth)acrylate groups (Cramer & Bowman, 2001; Hoyle & Bowman, 2010). Pentaerythritol tetrakis(3-mercaptopropionate) (PETMP), which contains four thiol groups, can therefore act as a multifunctional crosslinker in PEG-based networks. Burke et al. (2019) photopolymerized PEG dimethacrylate with a series of thiols under UV irradiation and found that PETMP formed hydrogels, whereas mercaptoacetate-based thiols did not copolymerize; incorporating PETMP also reduced the swelling ratio and stiffness relative to PEG dimethacrylate alone. These results indicate that thiol structure and functionality govern both network formation and the properties of the resulting hydrogel. UV photopolymerization is attractive for hydrogel preparation because it enables rapid network formation under comparatively mild conditions, and it allows functional comonomers to be incorporated to tailor the chemical environment of the network.

Introducing ionizable groups provides an additional means of tuning hydrogel–adsorbate interactions. Anionic functionalities such as carboxylate (–COO−) and sulfonate (–SO3−) groups are commonly incorporated into hydrogel networks to enhance the adsorption of cationic dyes through electrostatic attraction and ion-exchange interactions (Nasser, Thamer & Altaleb, 2025), and phosphorus-containing groups offer an alternative ionizable functionality (Nayl et al., 2026). Bis[2-(methacryloyloxy)ethyl] phosphate (BMEP) combines two polymerizable methacrylate groups with a phosphate moiety bearing an acidic P–OH group. BMEP was employed as a crosslinker in poly(vinylphosphonic acid) (PVPA) hydrogels developed for the adsorption of cationic MB, in which the acidic phosphorus-containing groups promoted interactions with MB, and the adsorption data followed pseudo-second-order kinetics and Langmuir-type behavior (Anil et al., 2020).

Previous work has thus examined, separately, PEG-based networks crosslinked with multifunctional thiols such as PETMP (Burke et al., 2019) and BMEP-containing phosphate-functional networks for MB adsorption (Anil et al., 2020). These systems differ in an important respect. In PVPA–BMEP hydrogels, BMEP crosslinks a polymer that already carries a high density of phosphonic acid groups, whereas in a PEG-based network, the ionizable phosphate functionality is introduced by BMEP into an otherwise non-ionic matrix. Whether BMEP-derived phosphate functionality can promote MB uptake within a UV-curable PEG–thiol network has not been addressed in the studies cited above.

Accordingly, the present study investigates a UV-photopolymerized poly(ethylene glycol) diacrylate (PEGDA)/PETMP/BMEP hydrogel as a functional adsorbent for the removal of MB from aqueous media. PEGDA serves as the PEG-based network-forming component, PETMP as a tetrafunctional thiol crosslinker, and BMEP as a reactive phosphate-containing comonomer. We hypothesized that the acidic P–OH groups of BMEP, which can ionize in aqueous media, would provide anionic sites for electrostatic interaction with MB^+. To compare the phosphate-containing formulation with a BMEP-free network, the BMEP-containing hydrogel was compared with a BMEP-free PEGDA/PETMP control that had the same PEGDA-to-solvent ratio and thiol:(meth)acrylate molar ratio and was prepared under the same processing and UV-curing conditions. Both hydrogels were characterized by Fourier-transform infrared (FTIR) spectroscopy, thermogravimetric analysis (TGA), and swelling measurements; dried Hfunc was also examined by scanning electron microscopy (SEM). MB removal was evaluated by monitoring the residual concentration by UV-Vis spectrophotometry as a function of contact time. This approach aims to establish a simple UV-curable phosphate-functional hydrogel platform

with potential relevance to colored aqueous streams associated with printing and related processes.

2. Methods

2.1. Materials

Poly(ethylene glycol) diacrylate (PEGDA, Mn ≈ 700 g mol^{-1}), pentaerythritol tetrakis(3-mercaptopropionate) (PETMP), bis[2-(methacryloyloxy)ethyl] phosphate (BMEP), and 2-hydroxy-2-methylpropiophenone (HMPP, photoinitiator) were used for hydrogel preparation. Methylene blue (MB) was used as a model cationic dye. Deionized water and ethanol were used as solvents. All reagents were purchased from Sigma-Aldrich and Merck.

2.2. Hydrogel preparation

Precursor solutions were prepared in water/ethanol (5:1, v/v) with the amounts given in Table 1. Deionized water and ethanol were mixed first, followed by PEGDA and BMEP (for the BMEP-containing formulation only), HMPP, and, finally, PETMP. The mixtures were homogenized, cast into the same Teflon mold, and irradiated with UV light for 5 min using a Luzchem Expo exposure panel equipped with six 8-W T5 LZC-UVA-367 lamps (λmax ≈ 367 nm) at a sample-to-lamp distance of 15 cm. After photopolymerization, the hydrogels were removed from the mold, washed thoroughly with deionized water to remove soluble residual species, and dried in an oven at 40 °C for 4 h. Specimens of similar geometry and dry mass were cut from the resulting hydrogels for the swelling and adsorption experiments. The BMEP-containing and the BMEP-free hydrogels are referred to as H_{func} and $H_{control}$, respectively.

Table 1

Composition of the precursor solutions of H_{func} and $H_{control}$

Component	$H_{control}$ (BMEP-free)	H_{func} (BMEP-containing)
PEGDA (g)	2.4	7.2
PETMP (g)	0.656	2.64
BMEP (g)	-	1.128
HMPP (g)	0.112	0.336
Deionized water (mL)	4	12
Ethanol (mL)	0.8	2.4

Both formulations have the same PEGDA-to-solvent ratio (0.5 g per mL of solvent) and the same HMPP content relative to PEGDA (4.7 wt%). The molar ratio of thiol to (meth)acrylate groups is also the same in both (0.78:1, calculated with PEGDA Mn = 700 g mol^{-1}, PETMP 488.66 g mol^{-1}, and BMEP 322.25 g mol^{-1}). BMEP corresponds to 10.3 wt% of the monomers (PEGDA, PETMP, and BMEP). The PETMP amount was increased in H_{func} to account for the additional methacrylate groups supplied by BMEP and maintain the same thiol:(meth)acrylate molar ratio. This does not establish an identical network architecture or crosslink density.

2.3. Characterization

FTIR spectra of the dried hydrogels were recorded on a Shimadzu IRSpirit-X series spectrometer in attenuated total reflection (ATR) mode over 4000–600 cm^{-1} and are presented as transmittance. The fracture surfaces of dried H_{func} were sputter-coated with a 3 nm Au/Pd layer and examined with a QUANTA 400F field emission scanning electron microscope using an ETD detector at 30 kV. Thermogravimetric analysis (TGA) of the hydrogels was performed using a PerkinElmer TGA 4000 (USA). Samples were heated from 30 °C to 750 °C at a heating rate of 40 °C min^{-1} under a nitrogen flow of 20 mL min^{-1}. The derivative thermogravimetry (DTG) curve is the instrument derivative of the thermogravimetric (TG) curve, smoothed with a Savitzky–Golay filter (cubic polynomial, 10.5 °C window). $T_{10\%}$ and $T_{50\%}$ are the temperatures at which the mass fell to 90% and 50% of the initial mass, and the residue was taken at 740 °C.

2.4. Swelling measurements

The swelling behavior was determined gravimetrically. Prior to the measurements, the hydrogels were dried in an oven at 40 °C for 4 h and weighed (Wd). Each specimen was placed in a separate beaker containing 20 mL of deionized water. After 15 min, 30 min, 60 min, 4 h, and 24 h, the specimen was removed, the surface water was gently blotted with filter paper, and the swollen specimen was weighed (Wt) and returned to the same water. The swelling ratio was calculated as:

$$SR\ (\%) = (W_t - W_d) / W_d \times 100 \quad (1)$$

One specimen of each hydrogel is reported in Table 2 ($H_{control}$, 0.6294 g dry; H_{func}, 0.63 g dry) without standard deviations; $H_{control}$ was not weighed at 4 h.

2.5. MB adsorption experiments

A dry hydrogel specimen (0.6291 g for H_{func} and 0.6253 g for $H_{control}$) was placed in 50 mL of a 10 mg L^{-1} MB solution at room temperature without stirring. The pH of the solution was neither measured nor adjusted. At 5, 10, 20, 30, 60, and 120 min and at 24 h, a 3–4 mL aliquot was withdrawn while the hydrogel remained in the beaker throughout the experiment, and its absorbance was measured; the aliquots were not returned to the beaker. Filtration or centrifugation was not used because the hydrogel material remained in the beaker during sampling. An adsorbent-free control containing the same 10 mg L^{-1} MB solution was maintained for 24 h under the same light, temperature, and agitation conditions as

the hydrogel-containing samples; both were kept without stirring. Its color and absorbance at 664 nm were compared with those of the initial solution. Absorbance was measured using a Thermo Scientific GENESYS 150 UV–Vis spectrophotometer with a 1 cm quartz cuvette.

The MB concentration was determined from the absorbance at 664 nm, using deionized water as the blank. The calibration curve was prepared from standard solutions of 2, 4, 6, 8, and 10 mg L^{-1}. The 8 and 10 mg L^{-1} standards were measured after five-fold dilution (1 mL of solution + 4 mL of deionized water), so the concentrations in the cuvette were 1.6 and 2.0 mg L^{-1}; the 10 mg L^{-1} solution was also measured without dilution (A = 2.225), which is exactly five times its diluted reading (A = 0.445). The absorbance was proportional to the concentration over 1.6–10 mg L^{-1} (Figure 1), and the calibration line was forced through the origin:

$$A = a\, C_{cuv} \quad (2)$$

with a = 0.219 L mg^{-1} and R^2 = 0.997. The MB concentration in a sample was calculated as:

$$C_t = DF\, A_t / a \quad (3)$$

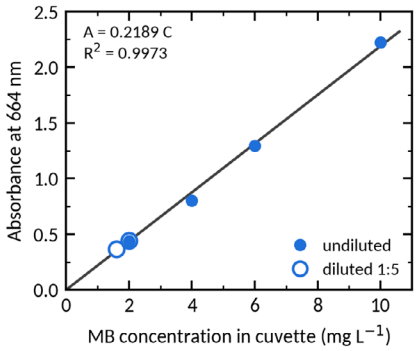
where A_t is the absorbance at 664 nm and DF is the dilution factor, $DF = (V_{sample} + V_{water}) / V_{sample}$; DF = 1 for undiluted samples and DF = 5 for 1 mL of sample + 4 mL of water. The initial concentration C0 was the value measured for the initial solution by the same procedure on the day of the experiment (10.2 mg L^{-1}, from the 10 mg L^{-1} solution measured without dilution; A = 2.225). MB removal and the amount adsorbed per gram of dry hydrogel (q_t) were calculated as:

$$R\,(\%) = (C_0 - C_t) / C_0 \times 100 \quad (4)$$

$$q_t = [C_0 V_0 - C_t V_t - \Sigma_{j<t}\, C_j V_{s,j}] / m_{gel} \quad (5)$$

$$V_t = V_0 - \Sigma_{j<t}\, V_{s,j} \quad (6)$$

where V_0 (L) is the solution volume when the hydrogel was added, $V_{s,j}$ (L) is the volume withdrawn at the j-th sampling, V_t (L) is the volume in the beaker before the t-th sampling, and m_{gel} (g) is the dry hydrogel mass. Because the withdrawn aliquots were not returned to the beaker, the MB removed with them is subtracted in Equation (5). R is a ratio of concentrations and does not depend on the withdrawn volume. Because individual aliquot volumes are specified only as a 3-4 mL range, the reported q_t values are approximate estimates based on 3.5 mL per aliquot. The removal percentages do not require this volume assumption.

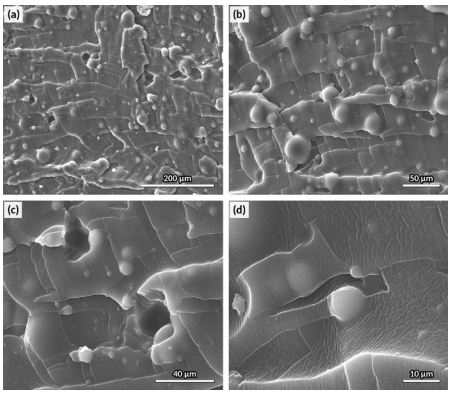


» **Figure 1:** *Calibration curve of MB at 664 nm. Open symbols: standards diluted 1:5 before measurement (8 and 10 mg L^{-1}); the 10 mg L^{-1} solution was also measured without dilution. Concentrations are those in the cuvette. Line: A = 0.219 C (R^2 = 0.997)*

3. Results

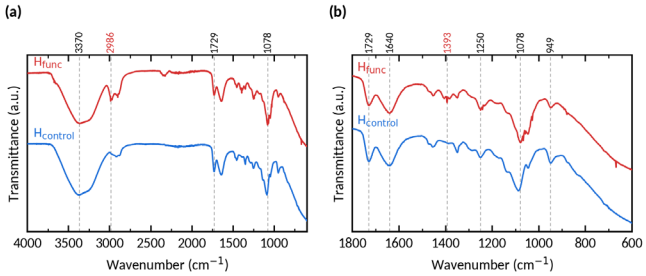
3.1. Morphology and chemical structure

SEM images of the fracture surface of the dried Hfunc at increasing magnification are shown in Figure 2. The surface is dense and continuous, with stepped fracture patterns consistent with fracture in a crosslinked network and scattered spherical features ranging from a few to a few tens of micrometers (Figure 2a,b). At higher magnification, cavities with smooth walls, spheres lying in or at the edge of the cavities, and a fine wrinkled texture on the fracture facets are visible (Figure 2c,d). No open, interconnected pores were observed in the dry state.



» **Figure 2:** *SEM images of the fracture surface of dried H_{func} at (a) 500×, (b) 1000×, (c) 2000×, and (d) 5000×*

The FTIR spectra of $H_{control}$ and H_{func} are shown in Figure 3. Both spectra were dominated by the bands of the PEGDA/PETMP network: a broad O–H stretching band cen-



» **Figure 3:** *FTIR spectra of $H_{control}$ and H_{func}: (a) 4000–600 cm⁻¹ and (b) 1800–600 cm⁻¹. The spectra are offset vertically for clarity*

tered at about 3370 cm⁻¹, C-H stretching bands between 3000 and 2850 cm⁻¹, the ester C=O stretching band at 1729 cm⁻¹, a band at 1640 cm⁻¹, ester C-O-C stretching near 1250 cm⁻¹ and an intense C-O-C stretching band of the PEG backbone at about 1085 cm⁻¹. Compared with $H_{control}$, the spectrum of H_{func} showed additional absorption near 2986 cm⁻¹, a distinct band at about 1393 cm⁻¹, a stronger band at 1250 cm⁻¹, and a broader and stronger C-O-C envelope whose maximum shifted from 1087 to 1078 cm⁻¹. The band at 1640 cm⁻¹ overlaps the bending vibration of water, and the S-H band of PETMP (about 2570 cm⁻¹) and the $=CH_2$ band of the acrylate groups (about 810 cm⁻¹) were not distinguishable from the baseline in either spectrum, so no conclusion on the conversion of the thiol and (meth)acrylate groups can be drawn. Phosphate-related vibrations may overlap the ester and ether bands in the fingerprint region, and ATR intensities depend on sample contact; the spectral differences are therefore treated as qualitative evidence rather than a quantitative measure of phosphate incorporation.

3.2. Thermal behavior

The TG and DTG curves of $H_{control}$ and H_{func} are presented in Figure 4. Both hydrogels exhibited only limited mass loss below 150 °C (1.6% for $H_{control}$ and 2.2% for H_{func}), followed by the principal degradation process at higher temperatures. H_{func} showed an earlier thermal degradation than the BMEP-free $H_{control}$, with T10% values of 337.3 and 375.1 °C and T50% values of 396.9 and 410.1 °C, respectively. The DTG minimum was less intense for H_{func} (−43.9 % min⁻¹) than for $H_{control}$ (−61.2 % min⁻¹), whereas the temperatures of maximum degradation rate were close (396 and 405 °C). The most pronounced difference between the two networks was observed at high temperature: H_{func} retained 7.12% of its initial mass at 740 °C, whereas $H_{control}$ left only 0.25% residue (Figure 4a, inset).

3.3. Swelling behavior

The swelling ratios of $H_{control}$ and H_{func} are given in Table 2 and Figure 5b (the swelling of H_{func} is illustrated by the photographs in Figure 5a). During the first hour, H_{func} showed substantially faster water uptake than $H_{control}$, reaching 34.9%, 44.4%, and 49.2% at 15, 30, and 60 min, respectively, compared with 3.6%, 4.5%, and 11.5% for $H_{control}$. H_{func} reached 54.0% at 4 h. After 24 h, the swelling ratios reached 65.1% for H_{func} and 55.5% for $H_{control}$. Thus, the largest difference between the formulations was observed during the early stage of hydration. These results are based on a single specimen of each hydrogel and should be confirmed by replicate measurements.

Table 2

Swelling ratio (%) of one specimen of each hydrogel in deionized water (20 mL per specimen); – = not measured

Specimen	W_d (g)	15 min	30 min	60 min	4h	24h
$H_{control}$	0.6294	3.6	4.5	11.5	-	55.5
H_{func}	0.63	34.9	44.4	49.2	54.0	65.1

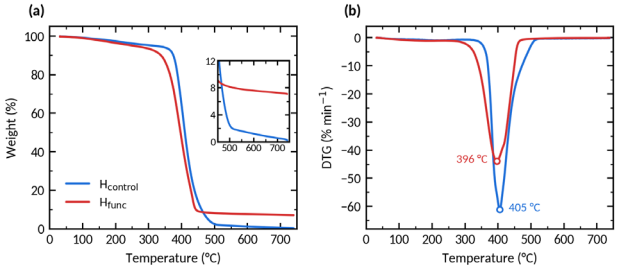
Table 3

Swelling ratio after 24 h in deionized water (one specimen of each hydrogel) and MB removal and estimated amount adsorbed (q) after 24 h. The q estimates assume 3.5 mL per withdrawn aliquot

Hydrogel	Swelling ratio at 24 h (%)	MB removal (%)	q at 24h (mg g⁻¹)
$H_{control}$	55.5	27.0	0.17
H_{func}	65.1	80.8	0.47

3.4. Methylene blue adsorption

Based on the calibration, MB removal by H_{func} increased from 13.3% at 5 min to 54.0% at 120 min and 80.8% at 24 h, whereas $H_{control}$ increased from 9.1% at 5 min to 16.5% at 120 min and 27.0% at 24 h (Figure 6b; Table 3). After correction for the decreasing solution volume and for MB removed in earlier aliquots, the estimated amounts adsorbed at 24 h, assuming 3.5 mL per withdrawn aliquot, were approximately 0.47 mg g⁻¹ for H_{func} and 0.17 mg g⁻¹ for $H_{control}$ (Figure 6c). After 24 h, the solution in contact with Hfunc was visibly lighter than that in contact with $H_{control}$, and the H_{func} hydrogel was intensely stained by the dye (Figure 6a). These values describe adsorption



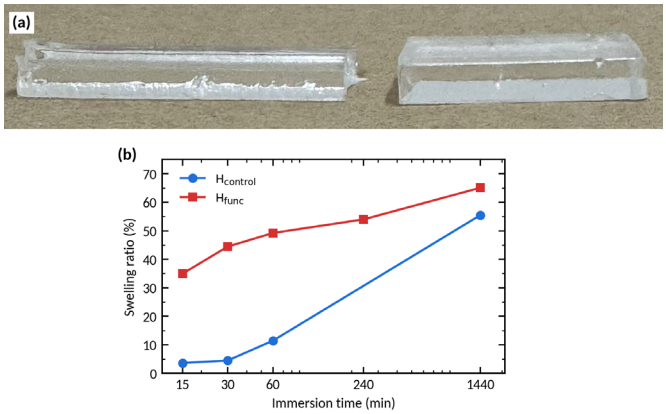
» **Figure 4:** *(a) TG and (b) DTG curves of $H_{control}$ and H_{func}; inset in (a): residue region.*

under the present experimental conditions and should not be interpreted as maximum adsorption capacities because only about 0.5 mg of MB was initially available in 50 mL of solution. All sample readings were within the 1.6–10 mg L^{-1} calibration range. The substantially greater MB removal observed for H_{func} relative to $H_{control}$ should be interpreted in light of the swelling behavior and the compositional differences between the two formulations. The adsorbent-free MB control showed no visible change in color, and its absorbance at 664 nm after 24 h under the same conditions was 2.198, compared with 2.225 for the initial solution (a decrease of about 1.2%); this change is much smaller than the decreases observed with the hydrogels, supporting the association of the concentration decrease with hydrogel presence; the removal values reported here were not corrected for it.

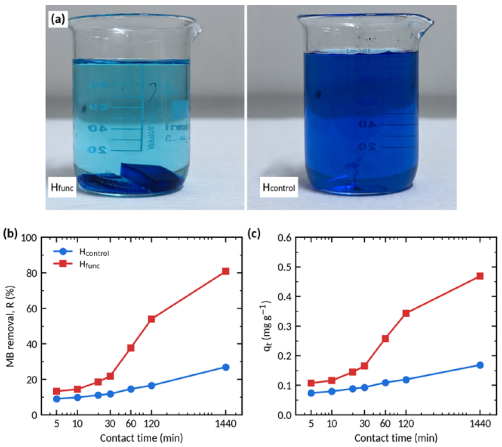
4. Discussion

The principal finding is the greater MB removal by the BMEP-containing formulation under the conditions examined: Hfunc removed 80.8% after 24 h, compared with 27.0% for $H_{control}$. The specimens were cut from hydrogels prepared in the same Teflon mold and had similar geometry and dry masses, reducing differences associated with initial specimen shape and adsorbent dose. The adsorbent-free MB control showed no visible color change, and its absorbance after 24 h was about 1.2% lower than the initial value, much smaller than the decreases observed with the hydrogels, supporting the association of the concentration decrease with the presence of hydrogels; the removal values were not corrected for this blank change. A possible contribution to the higher removal by H_{func} is electrostatic interaction between ionized BMEP-derived phosphate sites and cationic MB, as proposed for other phosphorus-containing hydrogels (Anil et al., 2020; Nayl et al., 2026). However, the pH and phosphate ionization were not determined, so the present results do not establish this mechanism. $H_{control}$ also showed MB uptake, indicating that phosphate functionality is not the sole possible contributor to dye retention in these networks.

The greater PETMP amount in Hfunc was required to maintain the same thiol:(meth)acrylate ratio after adding the methacrylate groups supplied by BMEP. Although this ratio and the PEGDA-to-solvent ratio were matched, the formulations differed in the PETMP-to-PEGDA mass ratio (0.37 versus 0.27 g g^{-1}) and total monomer content. Equal functional-group ratios do not establish equal crosslink densities or network structures (Cramer & Bowman, 2001). Consequently, the comparison demonstrates a formulation-level difference rather



» **Figure 5:** *(a) Photographs illustrating the swelling of Hfunc in a preliminary test: a dry piece (left; dried in an oven at 40 °C for 4 h) and a piece cut from the same specimen after 24 h in deionized water (right); (b) swelling ratios of $H_{control}$ and H_{func} (one specimen of each) in deionized water as a function of immersion time; lines connect the measured points*



» **Figure 6:** *(a) Photographs of the MB solutions after 24 h of contact with H_{func} (left) and $H_{control}$ (right) in a preliminary test (10 mg L^{-1} MB, ≈0.63 g of dry hydrogel); (b) MB removal and (c) estimated amount of MB adsorbed, q_t, by $H_{control}$ and H_{func} as a function of contact time (50 mL of 10 mg L^{-1} MB solution; 0.6253 g and 0.6291 g of dry hydrogel, respectively). The q_t values assume 3.5 mL per withdrawn aliquot*

than isolating the effect of phosphate groups. Burke et al. (2019) reported changes in swelling and stiffness upon incorporating PETMP into PEG dimethacrylate hydrogels, illustrating the relevance of thiol-containing network composition, although their system differs from the present PEGDA-based formulations.

H_{func} exhibited faster early hydration and a higher 24 h swelling ratio than $H_{control}$ (65.1% versus 55.5%). The swelling and removal values did not increase proportionally across the formulations, and no direct quantitative relationship can be inferred because swelling was measured in deionized water, and dye uptake in the MB solution. H_{func} continued to remove MB between 2 and 24 h, with MB removal increasing from 54.0% to 80.8%, despite substantial water uptake during the first hour in the separate swelling experiment. This is consistent with dye uptake extending beyond the early hydration period, without establishing a diffusion-controlled mechanism or an equilibrium endpoint.

The dense appearance of the dried H_{func} surface does not contradict its ability to absorb water. Dry-state SEM describes the observed fracture surface rather than the hydrated network, and neither SEM nor the bulk swelling ratio determines the wet-state mesh size or pore connectivity. The spherical features and cavities may reflect trapped air or heterogeneity formed during photopolymerization, but their origin cannot be resolved from these images. They should not be interpreted as evidence of an interconnected porous structure. Because SEM was performed only for H_{func}, the effect of formulation on morphology cannot be assessed by comparison with $H_{control}$.

The BMEP-containing formulation showed earlier thermal degradation and a greater residual mass at 740 °C. Related phosphate-containing UV-cured acrylate systems (Liang & Shi, 2004; Chen et al., 2008a; Chen et al., 2008b; Chen, Song & Hu, 2010) have shown degradation pathways involving phosphate decomposition and condensed-phase char formation (Liang & Shi, 2004; Chen et al., 2008a; Chen et al., 2008b). These coating systems offer a possible interpretation of the residual mass difference rather than evidence that the same mechanism occurred in the present hydrogels. Together, the FTIR and TGA results support physicochemical differences between the formulations, but do not independently establish covalent incorporation of BMEP, phosphorus content, or residue composition. TGA is used here as a complementary characterization method; high-temperature degradation behavior does not establish stability or resistance to leaching under aqueous adsorption conditions.

The removal percentages were obtained at an initial dry hydrogel dose of approximately 12.6 g L^{-1} and should be interpreted in that context. Only about 0.5 mg of MB was initially present, so the estimated 24 h uptake values of 0.47 and 0.17 mg g^{-1} do not represent maximum adsorption capacities. Repeated withdrawal of aliquots increased the hydrogel-to-solution ratio; the mass-balance calculation corrects for sampled dye and declining volume, while uncertainty in individual aliquot volumes limits the precision of qt. One adsorption time series and one swelling specimen per formulation are reported. Replicate measurements, controlled-pH experiments, and a range of initial concentrations are needed to distinguish chemical affinity from network effects and assess capacity. The printing-related relevance is therefore a motivation for future testing with actual wastewater and pigment-containing streams; the present experiments establish comparative removal of a model cationic dye in solution.

5. Conclusions

A UV-photopolymerized PEGDA/PETMP/BMEP hydrogel was prepared and evaluated for the removal of the model cationic dye methylene blue. With specimens of similar geometry and dry mass, H_{func} showed 80.8% removal after 24 h compared with 27.0% for the BMEP-free $H_{control}$; the adsorbent-free MB solution showed no visible change in color, and its absorbance decreased by only about 1.2% under the same conditions. H_{func} also showed faster initial hydration and a higher 24 h swelling ratio, while FTIR and TGA provided complementary evidence of physicochemical differences between the formulations. These findings support further study of UV-curable phosphate-containing networks for cationic-dye removal, while the specific role of phosphate groups, adsorption capacity, and performance in printing wastewater require further investigation.

6. References

Anil, I., Gunday, S.T., Bozkurt, A. and Alagha, O. (2020) 'Design of crosslinked hydrogels comprising poly(vinylphosphonic acid) and bis[2-(methacryloyloxy)ethyl] phosphate as an efficient adsorbent for wastewater dye removal', *Nanomaterials*, 10(1), 131. DOI: 10.3390/nano10010131

Burke, G., Cao, Z., Devine, D.M. and Major, I. (2019) 'Preparation of biodegradable polyethylene glycol dimethacrylate hydrogels via thiol-ene chemistry', *Polymers*, 11(8), 1339. DOI: 10.3390/polym11081339

Chen, X., Hu, Y., Song, L. and Xing, W. (2008a) 'Combustion and thermal behavior of polyurethane acrylate modified with a phosphorus monomer', *Journal of Fire Sciences*, 26(2), pp. 93–108. DOI: 10.1177/0734904107083863

Chen, X., Hu, Y., Song, L. and Xing, W. (2008b) 'Thermal properties and combustion behaviors of UV-cured phosphate triacrylate/star poly(urethane acrylate) oligomer blends', *Polymers for Advanced Technologies*, 19(5), pp. 393–398. DOI: 10.1002/pat.1022

Chen, X., Song, L. and Hu, Y. (2010) 'Flammability and thermal degradation of epoxy acrylate modified with phosphorus-containing compounds', *Journal of Applied Polymer Science*, 115(6), pp. 3332–3338. DOI: 10.1002/app.30477

Cramer, N.B. and Bowman, C.N. (2001) 'Kinetics of thiol–ene and thiol–acrylate photopolymerizations with real-time Fourier transform infrared', *Journal of Polymer Science Part A: Polymer Chemistry*, 39(19), pp. 3311–3319. DOI: 10.1002/pola.1314

Hoyle, C.E. and Bowman, C.N. (2010) 'Thiol–ene click chemistry', *Angewandte Chemie International Edition*, 49(9), pp. 1540–1573. DOI: 10.1002/anie.200903924

Kara, F., Birtane, H., Kandirmaz, E.A. and Cigil, A.B. (2026) 'A sustainable approach to ink colorant removal using modified cellulose from waste-paper', *Polymer Engineering & Science*, 66(6), pp. 4738–4752. DOI: 10.1002/pen.70537

Liang, H. and Shi, W. (2004) 'Thermal behaviour and degradation mechanism of phosphate di/triacrylate used for UV curable flame-retardant coatings', *Polymer Degradation and Stability*, 84(3), pp. 525–532. DOI: 10.1016/j.polymdegradstab.2003.11.006

Nasser, A.M., Thamer, B.M. and Altaleb, H.A. (2025) 'Chitosan-g-poly (styrene sulfonate) hydrogel with crosslinked polymeric for the efficient remediation of cationic dyeing wastewater', *Journal of King Saud University – Science*, 37(6), 7382025. DOI: 10.25259/JKSUS_738_2025

Nayl, A.A., Ahmed, I.M., Alsahli, S.A., Arafa, W.A.A., AlShammari, K.L., Gomha, S.M., Alanazi, M.D., Doma, A.S., AlHazmi, A.F.A., Bräse, S. and Abd-Elhamid, A.I. (2026) 'Highly selective removal of cationic dye using a novel synthesized polyacrylic polyacrylamide phosphate (PAA@PAm@P) hydrogel', *Scientific Reports*, 16(1), 19564. DOI: 10.1038/s41598-026-56160-x

Pereira, A.G.B., Rodrigues, F.H.A., Paulino, A.T., Martins, A.F. and Fajardo, A.R. (2021) 'Recent advances on composite hydrogels designed for the remediation of dye-contaminated water and wastewater: a review', *Journal of Cleaner Production*, 284, 124703. DOI: 10.1016/j.jclepro.2020.124703

Rafatullah, M., Sulaiman, O., Hashim, R. and Ahmad, A. (2010) 'Adsorption of methylene blue on low-cost adsorbents: a review', *Journal of Hazardous Materials*, 177(1–3), pp. 70–80. DOI: 10.1016/j.jhazmat.2009.12.047

Yang, Y., Zhu, Q., Peng, X., Sun, J., Li, C., Zhang, X., Zhang, H., Chen, J., Zhou, X., Zeng, H. and Zhang, Y. (2022) 'Hydrogels for the removal of the methylene blue dye from wastewater: a review', *Environmental Chemistry Letters*, 20(4), pp. 2665–2685. DOI: 10.1007/s10311-022-01414-z

© 2026 Authors. Published by the University of Novi Sad, Faculty of Technical Sciences, Department of Graphic Engineering and Design. This article is an open access article distributed under the terms and conditions of the Creative Commons Attribution license 4.0 Serbia (http://creativecommons.org/licenses/by/4.0/rs/).